Comput. Methods Appl. Mech. Engrg. 241–244 (2012) 38–51

Contents lists available at SciVerse ScienceDirect

Comput. Methods Appl. Mech. Engrg.

journal homepage: www.elsevier.com/locate/cma

Avoiding shear locking for the Timoshenko beam problem via isogeometric collocation methods

L. Beirão da Veiga [a,b,*], C. Lovadina [c,b], A. Reali [d,b]

[a] Mathematics Department "F. Enriques", University of Milan, Italy
[b] IMATI–CNR, Pavia, Italy
[c] Mathematics Department, University of Pavia, Italy
[d] Department of Civil Engineering and Architecture, University of Pavia, Italy

ARTICLE INFO

Article history:
Received 23 January 2012
Received in revised form 24 May 2012
Accepted 26 May 2012
Available online 9 June 2012

Keywords:
Isogeometric analysis
Collocation methods
B-splines
Timoshenko beam

ABSTRACT

In this work we study isogeometric collocation methods for the Timoshenko beam problem, considering both mixed and displacement-based formulations. In particular, we show that locking-free solutions are obtained for mixed methods independently on the approximation degrees selected for the unknown fields. Moreover, several numerical tests are provided in order to support our theoretical results and to show the good behavior and the flexibility of isogeometric collocation methods in this context.

1. Introduction

Isogeometric analysis (IGA) is a recent idea, firstly introduced by Hughes et al. [13,19], to fill the gap between computational mechanics and computer aided design (CAD). The key feature of IGA is to extend the finite element method (FEM) representing the geometry by spline functions typically used by CAD systems, and then invoking the isoparametric concept to define field variables. As a consequence, the computational domain exactly reproduces the CAD description of the physical domain. Moreover, further research on IGA has shown that the high regularity properties of the employed functions leads in many cases to a better accuracy-to-computational-effort ratio than standard FEM (cf., e.g. [14,20,23]). On these bases, many applications of IGA in different fields have been studied and implemented, highlighting the unique properties and advantages of this approach (see, among others, [1,2,5–12,15,17,21,25]).

Within the framework of IGA, collocation methods have been recently proposed in [3], constituting an appealing high-order low-cost alternative to standard Galerkin approaches. Such techniques have also been successfully applied to elastostatics and explicit elasodynamics [4]. Among the many interesting Computational Mechanics applications which can be successfully tackled by means of isogeometric collocation methods, the approximation of thin structure problems looks particularly promising; therefore, the aim of this paper is to initiate the study of this topic.

We here focus on the simple case of an initially straight planar Timoshenko beam. Despite its simplicity, the numerical approximation of this problem often presents some difficulties, especially when dealing with FEM in connection with low-order schemes. Indeed, one has to avoid the so-called *shear locking phenomenon*, which arises when the beam thickness parameter becomes "small". Within the FEM framework, several options to overcome *shear locking* are nowadays well-established. For example, ad-hoc reduced integration of the shear energy term can be used. Alternatively (and, sometimes, equivalently), the employment of discrete schemes based on a suitable *mixed formulation* can be of great advantage. However, the use of a mixed formulation does not solve the problem by itself: the discrete approximation spaces must be carefully chosen to avoid shear locking, and to prevent the occurrence *spurious modes*.

On the contrary, in this paper we show that suitable isogeometric collocation methods can be designed, leading to *locking-free schemes without the need of any compatibility condition between the selected discrete spaces*. Therefore, the convergence behaviour, *uniform in the thickness parameter*, is dictated only by the approximation features of the discrete spaces. We note that this very appealing property is deeply linked to the collocation method adopted and not only a consequence of the isogeometric approach.

An outline of the paper is the following. In Section 2 we briefly review the basics of isogeometric analysis, focusing on the one-dimensional case. In Section 3 we present the Timoshenko planar

* Corresponding author. Address: Mathematics Department "F. Enriques", University of Milan, Via Saldini 50, 20133 Milan, Italy. Tel.: +39 02 50316081.
E-mail address: lourenco.beirao@unimi.it (L. Beirão da Veiga).

0045-7825/$ - see front matter © 2012 Elsevier B.V. All rights reserved.
http://dx.doi.org/10.1016/j.cma.2012.05.020

beam problem, by considering a suitable mixed formulation, as well as the standard displacement-based equations. In Section 4 we propose our isogeometric collocation methods, based on the different formulations considered in Section 3. Section 5 is devoted to a rigorous error analysis for the collocation methods based on the mixed formulation. As already mentioned, our main result (cf. Theorem 5.1) states that the proposed schemes are *convergent and locking-free irrespective of any balancing among the selected discrete spaces*. We also identify that, in some cases, mixed methods are in fact equivalent to suitable displacement-based schemes. In Section 6 we report an extensive set of numerical tests, performed by means of the proposed methods. The presented numerical results clearly show the appealing features of our isogeometric collocation approach. Finally, in Section 7 we draw our conclusions.

In the following C will indicate a generic positive constant independent of the knot vectors, possibly different at each occurrence. Finally, we will denote with $L^\infty(\omega)$ and

$$W^{s,\infty}(\omega) = \left\{ v \in L^\infty(\omega) : \frac{d^m v}{dx^m} \in L^\infty(\omega)\ \forall m = 0, 1, \ldots, s \right\}, \quad s \in \mathbb{N},$$

the usual functional spaces, defined on a generic interval ω. When $\omega = (a, b)$, we simply write L^∞ and $W^{s,\infty}$.

2. B-spline-based isogeometric analysis

The aim of this section is to present a short description of B-splines, followed by a simple discussion on the basics of isogeometric analysis.

2.1. B-splines

A *knot vector* is a set of non-decreasing real numbers representing coordinates in the parametric space $[0, 1]$:

$$\{\xi_1 = 0, \ldots, \xi_{n+p+1} = 1\}, \tag{1}$$

where p is the order of the B-spline and n is the number of basis functions (and control points) necessary to describe it. The interval $[\xi_1, \xi_{n+p+1}]$ is called a *patch*. A knot vector is said to be *uniform* if its knots are uniformly-spaced and *non-uniform* otherwise; it is said to be *open* if its first and last knots have multiplicity $p + 1$. In what follows, we always employ open knot vectors. Basis functions formed from open knot vectors are interpolatory at the ends of the parametric interval $[0, 1]$ but are not, in general, interpolatory at interior knots.

Given a knot vector, univariate B-spline basis functions are defined recursively starting with $p = 0$ (piecewise constants)

$$N_{i,0}(\xi) = \begin{cases} 1 & \text{if } \xi_i \leqslant \xi < \xi_{i+1} \\ 0 & \text{otherwise.} \end{cases} \tag{2}$$

For $p > 1$:

$$N_{i,p}(\xi) = \begin{cases} \frac{\xi - \xi_i}{\xi_{i+p} - \xi_i} N_{i,p-1}(\xi) + \frac{\xi_{i+p+1} - \xi}{\xi_{i+p+1} - \xi_{i+1}} N_{i+1,p-1}(\xi) & \text{if } \xi_i \leqslant \xi < \xi_{i+p+1} \\ 0 & \text{otherwise,} \end{cases} \tag{3}$$

where, in (3), we adopt the convention $0/0 = 0$.

In Fig. 1 we present an example consisting of $n = 9$ cubic basis functions generated from the open knot vector $\{0, 0, 0, 0, 1/6, 1/3, 1/2, 2/3, 5/6, 1, 1, 1, 1\}$.

If internal knots are not repeated, B-spline basis functions are C^{p-1}-continuous. If a knot has multiplicity k, the basis is C^{p-k}-continuous at that knot. In particular, when a knot has multiplicity p, the basis is C^0 and interpolates the control point at that location. We define

$$\mathcal{S}_n = \text{span}\{N_{i,p}(\xi), i = 1, \ldots, n\} \tag{4}$$

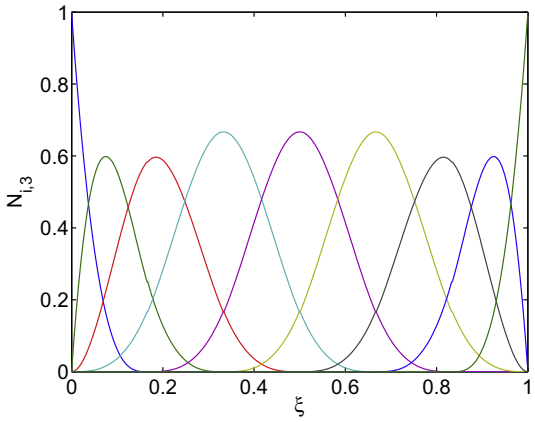

Fig. 1. Cubic basis functions formed from the open knot vector $\{0,0,0,0,1/6,1/3,1/2,2/3,5/6,1,1,1,1\}$.

the spline space spanned by the basis functions $N_{i,p}(\xi)$. Following the isogeometric approach, the space of B-spline functions defined on a generic interval $[a, b]$ is given by:

$$\mathcal{V}_n = \text{span}\{N_{i,p} \circ F^{-1}, i = 1, \ldots, n\}, \tag{5}$$

where $x = F(\xi) = a + (b - a)\xi$ is the linear parametrization which maps $[0, 1]$ onto $[a, b]$. We finally note that the images of the knots through the function F naturally define a partition of the interval (a, b), called the associated mesh $\mathcal{M}_h$, h being the mesh-size, i.e., the largest size of the elements in the mesh.

3. Timoshenko beam equations

We consider an initially straight, planar, elastic, and homogenous beam. The beam axis is assumed to occupy the interval $[a, b]$. Following the Timoshenko model [24], we introduce two possible ways to describe the beam static problem.

3.1. Mixed formulation

We first introduce a mixed formulations, where the unknown variables are the displacements $v(x)$ (usually referred to as deflections), the rotations $\varphi(x)$, and the shear strain $\gamma(x)$. Assuming for simplicity, but without loss of generality, clamped boundary conditions, the equations to be solved are the following:

$$\begin{cases} \kappa GA\gamma'(x) = p(x), & x \in]a, b[\\ -EI\varphi''(x) + \kappa GA\gamma(x) = 0, & x \in]a, b[\\ v'(x) + \varphi(x) - \gamma(x) = 0, & x \in]a, b[\\ v(a) = v(b) = 0, & \\ \varphi(a) = \varphi(b) = 0, & \end{cases} \tag{6}$$

where G and E are respectively the shear and Young's moduli, $p(x)$ is the transversal load per unit length, κ is the so-called shear correction factor, and A and I are the cross section area and the relevant moment of inertia, respectively. In particular, considering for simplicity a rectangular cross-section of width d and depth t (usually referred to as beam thickness), we have $\kappa = 5/6, A = dt$, and $I = dt^3/12$.

For analysis purposes, we rewrite the equations above in a more convenient scaled form, where the unknowns are again the transversal displacements $v(x)$ and the rotations $\varphi(x)$, plus a variable, $\tau(x)$, associated to shear stresses. In this case, the equations to be solved read:

$$\begin{cases} \tau'(x) = \alpha q(x), & x \in]a,b[\\ -\varphi''(x) + \tau(x) = 0, & x \in]a,b[\\ v'(x) + \varphi(x) - \alpha^{-1}t^2\tau(x) = 0, & x \in]a,b[\\ v(a) = v(b) = 0, \\ \varphi(a) = \varphi(b) = 0. \end{cases} \tag{7}$$

In (7), we have set $q(x) = -\frac{6f_v(x)}{5Gt^2}$ and $\alpha = 10\frac{G}{E}, f_v(x) = \frac{p(x)}{A}$ being the transversal load per unit volume.

3.2. Displacement-based formulation

Eliminating the shear strain using the third equation of (6), one gets the following displacement-based formulation, where the unknowns are the transversal displacements $v(x)$ and the rotations $\varphi(x)$:

$$\begin{cases} \kappa GA(v''(x) + \varphi'(x)) = -p(x), & x \in]a,b[\\ -EI\varphi''(x) + \kappa GA(v'(x) + \varphi(x)) = 0, & x \in]a,b[\\ v(a) = v(b) = 0, \\ \varphi(a) = \varphi(b) = 0. \end{cases} \tag{8}$$

In a scaled form similar to (7), the equations above read:

$$\begin{cases} t^{-2}(v''(x) + \varphi'(x)) = q(x), & x \in]a,b[\\ -\varphi''(x) + \alpha t^{-2}(v'(x) + \varphi(x)) = 0, & x \in]a,b[\\ v(a) = v(b) = 0, \\ \varphi(a) = \varphi(b) = 0. \end{cases} \tag{9}$$

4. Isogeometric collocation methods for the Timoshenko beam

In this Section, we present our collocation methods for the Timoshenko beam, which are implemented in the spirit of isogeometric collocation methods, as introduced in [3] and further developed in [4].

Before proceeding, we need to introduce the B-spline space $\Phi_h \subset C^2(a,b)$, used for the rotation approximation, and associated with the knot vector

$$\{\xi_1^{\varphi} = 0, \dots, \xi_{n_v+p_v+3}^{\varphi} = 1\}. \tag{10}$$

Accordingly, we set (cf. (4) and (5)):

$$\Phi_h = \mathcal{V}_{n_\varphi+2}. \tag{11}$$

Analogously, we introduce the B-spline space

$$V_h = \mathcal{V}_{n_v+2} \subset C^2(a,b), \tag{12}$$

used for the deflection approximation, and associated with the knot vector

$$\{\xi_1^{v} = 0, \dots, \xi_{n_v+p_v+3}^{v} = 1\}. \tag{13}$$

Finally, we define the B-spline space

$$\Gamma_h = \mathcal{V}_{n_\tau} \subset C^1(a,b), \tag{14}$$

used for the shear stress approximation, and associated with the knot vector

$$\{\xi_1^{\tau} = 0, \dots, \xi_{n_\tau+p_\tau+1}^{\tau} = 1\}. \tag{15}$$

We notice that it holds

$$\dim(\Phi_h) = n_\varphi + 2; \quad \dim(v_h) = n_v + 2; \quad \dim(\Gamma_h) = n_\tau. \tag{16}$$

Remark 4.1. Furthermore, we remark that the three knot vectors above induce, in principle, three different meshes:

$$\mathcal{M}_{h_\varphi}; \quad \mathcal{M}_{h_v}; \quad \mathcal{M}_{h_\tau},$$

with corresponding mesh-sizes h_φ, h_v, and h_τ. In the sequel, we will set $h = \max\{h_\varphi, h_v, h_\tau\}$. However, we notice that, in practical applications, the three meshes most often coincide.

In the sequel, we will also use the spaces of first and second derivatives:

$$\Phi_h'' =: \{\varphi_h'' : \varphi_h \in \Phi_h\}; \quad V_h' =: \{v_h' : v_h \in V_h\}; \quad \Gamma_h' =: \{\tau_h' := \tau_h \in \Gamma_h\}, \tag{17}$$

whose dimensions are obviously given by $\dim(\Phi_h'') = n_\varphi$, $\dim(V_h') = n_v + 1$, and $\dim(\Gamma_h\prime) = n_\tau$, see (16). Furthermore, we introduce suitable sets of collocation points in $[a,b]$:

$$\begin{cases} \mathcal{N}(\Phi_h'') = \{x_1, x_2, \dots, x_{n_\varphi}\}, \\ \mathcal{N}(V_h') = \{y_1, y_2, \dots, y_{nv+1}\}, \\ \mathcal{N}(\Gamma_h') = \{z_1, z_2, \dots, z_{n_\tau-1}\}. \end{cases} \tag{18}$$

We notice that it holds $\#(\mathcal{N}(\Phi_h'')) = \dim(\Phi_h) - 2$, $\#(\mathcal{N}(V_h')) = \dim(V_h) - 1$, and $\#(\mathcal{N}(\Gamma_h')) = \dim(\Gamma_h) - 1$. Therefore, we have (cf. (7)):

$$\begin{aligned} &(\#\mathcal{N}(\Phi_h'')) + (\#\mathcal{N}(V_h')) + (\#\mathcal{N}(\Gamma_h')) + (\#(\text{boundary conditions})) \\ &\quad = \dim(\Phi_h) + \dim(V_h) + \dim(\Gamma_h). \end{aligned} \tag{19}$$

Remark 4.2. The reason for introducing the notations $(\mathcal{N}(\Phi_h''))$, $\mathcal{N}(V_h')$, and $(\mathcal{N}(\Gamma_h')$ is the following. The chosen collocation points should be compatible with the existence of a *stable interpolating operator* on the *derivative* spaces $\Phi_h\prime\prime, V_h\prime$, and $\Gamma_h\prime$, respectively (see Assumption 5.1). We will discuss some possible practical choices of the collocation points later on in the paper.

4.1. Mixed discretizations

We now introduce our collocation method based on the mixed formulation (7). Given the finite dimensional spaces defined in (11), (12), and (14), together with the collocation points introduced in (18), the discretized problem reads as follows.

$$\begin{cases} \text{Find } (\varphi_h, v_h, \tau_h) \in \Phi_h \times V_h \times \Gamma_h \text{ such that :} \\ \tau_h'(z_i) = \alpha q(z_i), & z_i \in (\mathcal{N}(\Gamma_h')) \\ -\Phi_h''(x_j) + \tau_h(x_j) = 0, & x_j \in (\mathcal{N}(\Phi_h'')) \\ v_h'(y_k) + \Phi_h(y_k) - \alpha^{-1}t^2\tau_h(y_k) = 0, & y_k \in \mathcal{N}(V_h') \\ v_h(a) = v_h(b) = 0, \\ \varphi_h(a) = \varphi_h(b) = 0. \end{cases} \tag{20}$$

Notice that, according with (16) and (19), problem (20) is a linear system of $(n_\varphi + n_v + n_\tau + 4)$ equations for $(n_\varphi + n_v + n_\tau + 4)$ unknowns.

Different choices could also be made. For instance, one could think of considering the discrete equations:

$$\begin{cases} \text{Find } (\varphi_h, v_h, \tau_h) \in \Phi_h \times V_h \times \Gamma_h \text{ such that :} \\ \tau_h'(y_k) = \alpha q(y_k), & y_k \in \mathcal{N}(V_h') \\ -\varphi_h''(x_j) + \tau_h(x_j) = 0, & x_j \in (\mathcal{N}(\Phi_h'')) \\ v_h'(z_i) + \varphi_h(z_i) - \alpha^{-1}t^2\tau_h(z_i) = 0, & z_i \in (\mathcal{N}(\Gamma_h')) \\ v_h(a) = v_h(b) = 0, \\ \varphi_h(a) = \varphi_h(b) = 0. \end{cases} \tag{21}$$

Formulation (21) is obtained by simply swapping the collocation points for equations $(20)_{(1)}$ and $(20)_{(3)}$. This choice may be called *variational-like*, since it corresponds to the standard variational framework, where Eqs. $(21)_{(1)}$, $(21)_{(2)}$), and $(21)_{(3)}$ are weighted by deflection, rotation and shear deformation test functions, respectively (for more details see [4]).

In the sequel, we consider the more *"unusual"* formulation (20), since it leads to *locking-free schemes for every choice of discretization spaces*, and it is amenable to a rigorous error analysis, see Section 5. However, we notice that, in some cases, the two formulations (20) and (21) coincide. For example, this obviously occurs when $V_h = \Gamma_h$ and $\mathcal{N}(V_h') = \mathcal{N}(\Gamma_h')$, cf. Section 6.2.

4.2. Displacement-based discretizations

We now introduce our collocation method based on the displacement-based formulation (9). We need to introduce the space of the second derivatives of V_h:

$$V_h'' =: \{v_h'' : v_h \in V_h\},$$

together with suitable collocation points in $[a,b]$

$$\mathcal{N}(V_h'') = \{w_1, w_2, \dots, w_{nv}\} \quad (\text{cf. also Remark 4.2}). \tag{22}$$

We notice that it holds $\#(\mathcal{N}(V_h'')) = \dim(V_h) - 2$. Considering the finite dimensional spaces defined in (11), as well as the collocation points introduced in $(18)_1$, the discretized problem reads as follows:

$$\begin{cases} \text{Find } (\varphi_h, v_h) \in \Phi_h \times V_h \text{ such that :} \\ t^{-2}\big(v_h\prime\prime(w_j) + \varphi_h\prime(w_j)\big) = q(w_j), & w_j \in \mathcal{N}(V_h'') \\ -\varphi_h\prime\prime(x_k) + \alpha t^{-2}(v_h\prime(x_k) + \varphi_h(x_k)) = 0, & x_k \in \mathcal{N}(\Phi_h'') \\ v_h(a) = v_h(b) = 0, \\ \varphi_h(a) = \varphi_h(b) = 0. \end{cases} \tag{23}$$

Notice that problem (23) is a linear system of $(n_\varphi + n_v + 4)$ equations and $(n_\varphi + n_v + 4)$ unknowns. We also remark that formulation (23) corresponds to a *variational-like* choice, cf. Section 4.1.

Remark 4.3. We must note that the linear systems arising from collocation methods are in general non symmetric; the same happens for the formulation presented here. This may have implications, for instance, in vibration analysis since the eigenvalues are not, in principle, guaranteed to be real. However, the numerical tests performed in [3] have shown that real eigenvalues are in general expected.

5. Theoretical results

In this Section, we develop a theoretical analysis of the collocation method presented in Section 4.1, based on the *mixed formulation* of Section 3.1. The same analysis can be applied, in some cases, also to the *displacement-based* method, see Section 4.2, as detailed in Section 5.4.1.

We make the following fundamental assumption on the collocation points.

Assumption 5.1 (*Stable interpolation*). There exists a constant C_{int}, independent of the knot vectors, such that the following holds. For all functions θ, w, and r in $C^0(a,b)$ there exist unique interpolating functions

$$\begin{aligned} &\theta_{II}(x_j) = \theta(x_j), \quad \forall x_j \in \mathcal{N}(\Phi_h''), \quad \theta_{II} \in \Phi_h'', \\ &w_{III}(x_j) = w(x_j), \quad \forall z_i \in \mathcal{N}(V_h'), \quad w_{III} \in V_h', \\ &r_I(x_j) = r(x_j), \quad \forall y_k \in \mathcal{N}(\Gamma_h'), \quad r_I \in \Gamma_h', \end{aligned}$$

with the bounds

$$\begin{aligned} &\|\theta_{II}\|_{L^\infty} \leqslant C_{\text{int}} \|\theta\|_{L^\infty}, \\ &\|w_{III}\|_{L^\infty} \leqslant C_{\text{int}} \|w\|_{L^\infty}, \\ &\|r_I\|_{L^\infty} \leqslant C_{\text{int}} \|r\|_{L^\infty}. \end{aligned}$$

A discussion on possible practical collocation points satisfying Assumption 5.1 can be found in Section 5.4.

5.1. A useful splitting

Our starting point is the following splitting of the solution (φ, v, τ) to problem (7). Indeed, by linearity, we may write

$$\begin{cases} \varphi = \varphi_o + \tilde{\varphi} \\ v = v_o + \tilde{v} \\ \tau = \tau_o + \tilde{\tau} \end{cases} \tag{24}$$

where (φ_o, v_o, τ_o) is the solution to the problem:

$$\begin{cases} \tau_o'(x) = \alpha q(x), & x \in]a,b[\\ -\varphi_o''(x) + \tau_0(x) = 0, & x \in]a,b[\\ v_0'(x) + \varphi_0(x) - \alpha^{-1} t^2 \tau_0(x) = 0, & x \in]a,b[\\ \tau_0(a) = 0, v_0(b) = 0, \\ \varphi_0(a) = \varphi_0(b) = 0, \end{cases} \tag{25}$$

and $(\tilde{\varphi}, \tilde{v}, \tilde{\tau})$ is the solution to the problem:

$$\begin{cases} \tilde{\tau}'(x) = 0, & x \in]a,b[\\ -\tilde{\varphi}''(x) + \tilde{\tau}(x) = 0, & x \in]a,b[\\ \tilde{v}'(x) + \tilde{\varphi}(x) - \alpha^{-1} t^2 \tilde{\tau}(x) = 0, & x \in]a,b[\\ \tilde{v}(a) = -v_0(a), \tilde{v}(b) = 0 \\ \tilde{\varphi}(a) = \tilde{\varphi}(b) = 0. \end{cases} \tag{26}$$

An analogous spitting holds for the solution (Φ_h, v_h, τ_h) to problem (20). Indeed, we may write

$$\begin{cases} \varphi_h = \varphi_{0,h} + \tilde{\varphi}_h \\ v_h = v_{0,h} + \tilde{v}_h, \\ \tau_h = \tau_{0,h} + \tilde{\tau}_h \end{cases} \tag{27}$$

where $(\varphi_{0,h}, v_{0,h}, \tau_{0,h})$ is the solution to the problem:

$$\begin{cases} \text{Find } (\varphi_{0,h}, v_{0,h}, \tau_{0,h}) \in \Phi_h \times V_h \times \Gamma_h \text{ such that :} \\ \tau_{0,h}'(z_i) = \alpha q(z_i), & z_i \in (\mathcal{N}(\Gamma_h') \\ -\varphi_{0,h}''(x_j) + \tau_{0,h}(x_j) = 0, & x_j \in \mathcal{N}(\Phi_h'') \\ v_{0,h}'(y_k) + \varphi_{0,h}(y_k) - \alpha^{-1} t^2 \tau_{0,h}(y_k) = 0, & y_k \in \mathcal{N}(V_h') \\ \tau_{0,h}(a) = 0, v_{0,h}(b) = 0, \\ \varphi_{0,h}(a) = \varphi_{0,h}(b) = 0. \end{cases} \tag{28}$$

and $(\tilde{\varphi}_h, \tilde{v}_h, \tilde{\tau}_h)$ is the solution to the problem:

$$\begin{cases} \text{Find } (\tilde{\varphi}_h, \tilde{v}_h, \tilde{\tau}_h) \in \Phi_h \times V_h \times \Gamma_h \text{ such that :} \\ \tilde{\tau}_h'(z_i) = 0, & z_i \in \mathcal{N}(\tau_h') \\ -\tilde{\varphi}_h''(x_j) + \tilde{\tau}_h(x_j) = 0, & x_j \in (\mathcal{N}(\Phi_h'') \\ \tilde{v}_h'(y_k) + \tilde{\varphi}_h(y_k) - \alpha^{-1} t^2 \tilde{\tau}_h(y_k) = 0, & y_k \in \mathcal{N}(V_h') \\ \tilde{v}_h(a) = -v_{0,h}(a), \tilde{v}_h(b) = 0, \\ \tilde{\varphi}_h(a) = \tilde{\varphi}_h(b) = 0. \end{cases} \tag{29}$$

Accordingly, the error quantities $(\varphi - \varphi_h, v - v_h, \tau - \tau_h)$ can be split as

$$\begin{cases} \varphi - \varphi_h = (\varphi_0 - \varphi_{0,h}) + (\tilde{\varphi} - \tilde{\varphi}_h) \\ v - v_h = (v_0 - v_{0,h}) + (\tilde{v} - \tilde{v}_h) \\ \tau - \tau_h = (\tau_0 - \tau_{0,h}) + (\tilde{\tau} - \tilde{\tau}_h). \end{cases} \tag{30}$$

Therefore, the error analysis can be performed by estimating the errors arising from the discretizations of problems (25) and (26), respectively.

Remark 5.1. We notice that problem (29) can be considered an approximation of problem (26), also because of the presence of the approximated boundary datum $-v_{0,h}(a)$ in place of $-v_0(a)$.

5.2. Discretization error for problem (25)

In the following, we will denote by k_φ, k_ν, k_τ the regularity index k introduced in Section 2.1, respectively associated to each space Φ_h, V_h, Γ_h. Note that, for simplicity, we assume that such regularity index is the same for all knots in each of the three knot vectors defining the discrete spaces.

We will make use of the approximation Lemma below, which can be proved using exactly the same techniques as in [12].

Lemma 5.1. *Let $\mathcal{V}$ be any spline space with associated polynomial degree p, global regularity index k and maximum mesh-size h. Then, there exists a projection operator $\Pi : L^\infty(a,b) \to \mathcal{V}$ such that, for all functions $f \in C^k(a,b)$ that satisfy $f|_E \in W^{m,\infty}(E)$ for all elements E of the mesh $\mathcal{M}_h$, it holds, for $0 \leqslant m \leqslant p+1$:*

$$\|f - \Pi f\|_{L^\infty} \leqslant C_A h^m \max_{E\in\mathcal{M}_h} |f|_{W^{m,\infty}(E)},$$

with the constant C_A independent of f and the mesh-size h.

We have the following corollary.

Corollary 5.1. Let $r \in C^{k_\tau - 1}(a,b)$ and such that $r|_E \in W^{m,\infty}(E)$ for all elements E of the mesh $\mathcal{M}_h$. Then for all $0 \leqslant s \leqslant m \leqslant p_{tau}$ it holds

$$\|\|r - r_I\|_{L^\infty} \leqslant C h^m \max_{E\in\mathcal{M}_h} |r|_{W^{m,\infty}(E)}.$$

where $r_I \in \Gamma_h\prime$ is defined in Assumption 5.1.

Proof. Let Π be the projection introduced in Lemma 5.1 for the space $\mathcal{V} = \Gamma_h\prime$. Note that the space $\Gamma_h\prime$ has polynomial order $p_\tau - 1$ and regularity index $k_\tau - 1$. By a triangle inequality and noting that $(\Pi r)_I = \Pi r$ it follows

$$\|r - r_I\|_{L^\infty} \leqslant \|r - \Pi r\|_{L^\infty} + \|(r - \Pi r)_I\|_{L^\infty}.$$

The proof then follows from the above bound first using Assumption 5.1 and then Lemma 5.1

$$\begin{aligned}\|r - r_I\|_{L^\infty} &\leqslant (1 + C_{\text{int}})\|r - \Pi r\|_{L^\infty} \\ &\leqslant (1 + C_{\text{int}}) C_A h^m \max_{E\in\mathcal{M}_h} |r|_{W^{m,\infty}(E)}. \qquad \square\end{aligned}$$

The same identical result holds for the space $V_h\prime$, simply substituting p_τ, k_τ with p_ν, k_ν in Corollary 5.1.

Moreover, the proof of the following corollary for the space $\Phi_h\prime\prime$ is analogous and, therefore, not detailed.

Corollary 5.2. Let $\theta \in C^{k_\phi - 2}(a,b)$ and such that $\theta|_E \in W^{m,\infty}(E)$ for all elements E of the mesh. Then for all $0 \leqslant m \leqslant p_p hi - 1$ it holds

$$\|\theta - \theta_{II}\|_{L^\infty} \leqslant C h^m |\theta|_{W^{m,\infty}},$$

where $\theta_{II} \in \Phi_h''$ is defined in Assumption 5.1.

We are now able to analyse the discretization error for problem (25). We start noting that, due to $(25)_1$ and $(28)_1$, it holds

$$\tau'_{0,h}(z_i) = \tau'_0(z_i), \quad \forall z_i \in \mathcal{N}(\Gamma'_h) \quad \Rightarrow \quad \tau'_{0,h} = (\tau'_0)_I,$$

where $(\tau'_0)_I \in \Gamma'_h$ is defined in Assumption 5.1.

Therefore, using first the above identity and the triangle inequality, then using Corollary 5.1, we get for all $0 \leqslant m \leqslant p_\tau$:

$$\begin{aligned}|\tau_0 - \tau_{h,0}|_{W^{1,\infty}} &= |\tau_0\prime - (\tau_0\prime)_I|_{L^\infty} \leqslant C h^m |\tau_0\prime|_{W^{m,\infty}} \\ &= C h^m |\tau_0|_{W^{m+1,\infty}}. \end{aligned} \tag{31}$$

Moreover, since $\tau_0(a) = \tau_{0,h}(a) = 0$, the Poincaré inequality yields

$$\|\tau_0 - \tau_{0,h}(a)\|_{L^\infty} \leqslant C h^m |\tau_0|_{W^{m+1,\infty}}. \tag{32}$$

Eqs. $(25)_2$ and $(28)_2$ yield respectively

$$\varphi_0'' = \tau_0, \quad \varphi_{0,h}'' = (\tau_{0,h})_{II}$$

where the symbol *II* denotes the interpolation introduced in Assumption 5.1.

Adding and subtracting $(\tau_0)_{II}$, using the above identities and the triangle inequality, we easily get:

$$\begin{aligned}|\varphi_0 - \varphi_{0,h}|_{W^{2,\infty}} &= \|\varphi_0\prime\prime - \varphi''_{0,h}\|_{L^\infty} \\ &\leqslant \|\tau_0 - (\tau_0)_{II}\|_{L^\infty} + \|(\tau_0)_{II} - (\tau_{0,h})_{II}\|_{L^\infty} \\ &= \|\tau_0 - (\tau_0)_{II}\|_{L^\infty} + \|(\tau_0 - \tau_{0,h})_{II}\|_{L^\infty}. \end{aligned} \tag{33}$$

The first term in the right hand side of (33) can be bounded applying Corollary 5.2, while a bound for the second term can be derived using Assumption 5.1 and then (32). We get, for all $0 \leqslant \overline{m} \leqslant p_\varphi - 1$ and $0 \leqslant m \leqslant p\tau$:

$$|\varphi_0 - \varphi_{0,h}|_{W^{2,\infty}} \leqslant C\Big(h^{\overline{m}} |\tau_0|_{W^{\overline{m},\infty}} + h^m |\tau_0|_{W^{m+1,\infty}}\Big). \tag{34}$$

Applying the above estimate with the choice $\overline{m} = p_\varphi - 1, m = p_\tau$, we obtain:

$$|\varphi_0 - \varphi_{0,h}|_{W^{2,\infty}} \leqslant C h^\gamma |\tau_0|_{W^{\gamma+1,\infty}} \tag{35}$$

with $\gamma = \min(p_\tau, p_\varphi - 1)$.

Due to the boundary conditions $\varphi_0(a) = \varphi_0(b) = \varphi_{0,h}(a) = \varphi_{0,h}(b) = 0$, a Poincaré inequality also gives

$$\|\varphi_0 - \varphi_{0,h}\|_{L^\infty} \leqslant C h^\gamma |\tau_0|_{W^{\gamma+1,\infty}}. \tag{36}$$

The same argument above can be applied also to the last two Eqs. $(25)_3$ and $(28)_3$. Note again that we have

$$\nu_0\prime = \varphi_0 + \alpha^{-1} t^2 \tau_0, \quad \nu'_{0,h} = \Big(\varphi_{0,h} + \alpha^{-1} t^2 \tau_{0,h}\Big)_{III}$$

where the symbol *III* denotes the interpolation introduced in Assumption 5.1. Using (31), (32), (35), and (36), since t is bounded from above, one easily gets

$$\begin{aligned}\|\nu_0 - \nu_{0,h}\|_{W^{1,\infty}} &\leqslant C h^{p_\nu}\big(t^2 |\tau_0|_{W^{p_\nu,\infty}} + |\tau_0|_{W^{p_\nu-2,\infty}}\big) \\ &\quad + C h^\gamma (t^2 + 1) |\tau_0|_{W^{\gamma+1,\infty}} \\ &\leqslant C h^\beta |\tau_0|_{W^{\beta+1,\infty}}, \end{aligned} \tag{37}$$

where $\beta := \min(p_\nu, p_\tau, p_\varphi - 1)$. Bounds (31), (35), and (37) give the error estimates for problem (25).

5.3. Discretization error for problem (26)

The solution to problem (26) can be analytically computed. Indeed, a direct computation shows that it holds:

$$\begin{cases} \tilde\varphi(x) = \frac{\nu_0(a)}{2c(t)} p_2(x); \\ \tilde\nu(x) = \frac{\nu_0(a)}{c(t)} \int_x^b \Big[\frac{p_2(\sigma)}{2} + \alpha^{-1} t^2\Big] \mathrm{d}\sigma; \\ \tilde\tau(x) = \frac{\nu_0(a)}{c(t)}, \end{cases} \tag{38}$$

where $p_2(x) = (x-a)(b-x)$, and $c(t) = (b-a)^3/48 + \alpha^{-1} t^2 (b-a)$.

We also notice that the solution of the discrete problem (29) can be analytically computed. Indeed, assuming $p_\nu \geqslant 3$, it is easy to check that:

$$\begin{cases} \tilde\varphi_h(x) = \frac{\nu_{0,h}(a)}{2c(t)} p_2(x); \\ \tilde\nu_h(x) = \frac{\nu_{0,h}(a)}{c(t)} \int_x^b \Big[\frac{p_2(\sigma)}{2} + \alpha^{-1} t^2\Big] \mathrm{d}\sigma; \\ \tilde\tau_h(x) = \frac{\nu_{0,h}(a)}{c(t)}. \end{cases} \tag{39}$$

As a consequence, we can express explicitly the errors:

$$\begin{cases} \tilde\varphi(x) - \tilde\varphi_h(x) = \frac{\nu_0(a) - \nu_{0,h}(a)}{2c(t)} p_2(x); \\ \tilde\nu(x) - \tilde\nu_h(x) = \frac{\nu_0(a) - \nu_{0,h}(a)}{c(t)} \int_x^b \Big[\frac{p_2(\sigma)}{2} + \alpha^{-1} t^2\Big] \mathrm{d}\sigma; \\ \tilde\tau(x) - \tilde\tau_h(x) = \frac{\nu_0(a) - \nu_{0,h}(a)}{c(t)}. \end{cases} \tag{40}$$

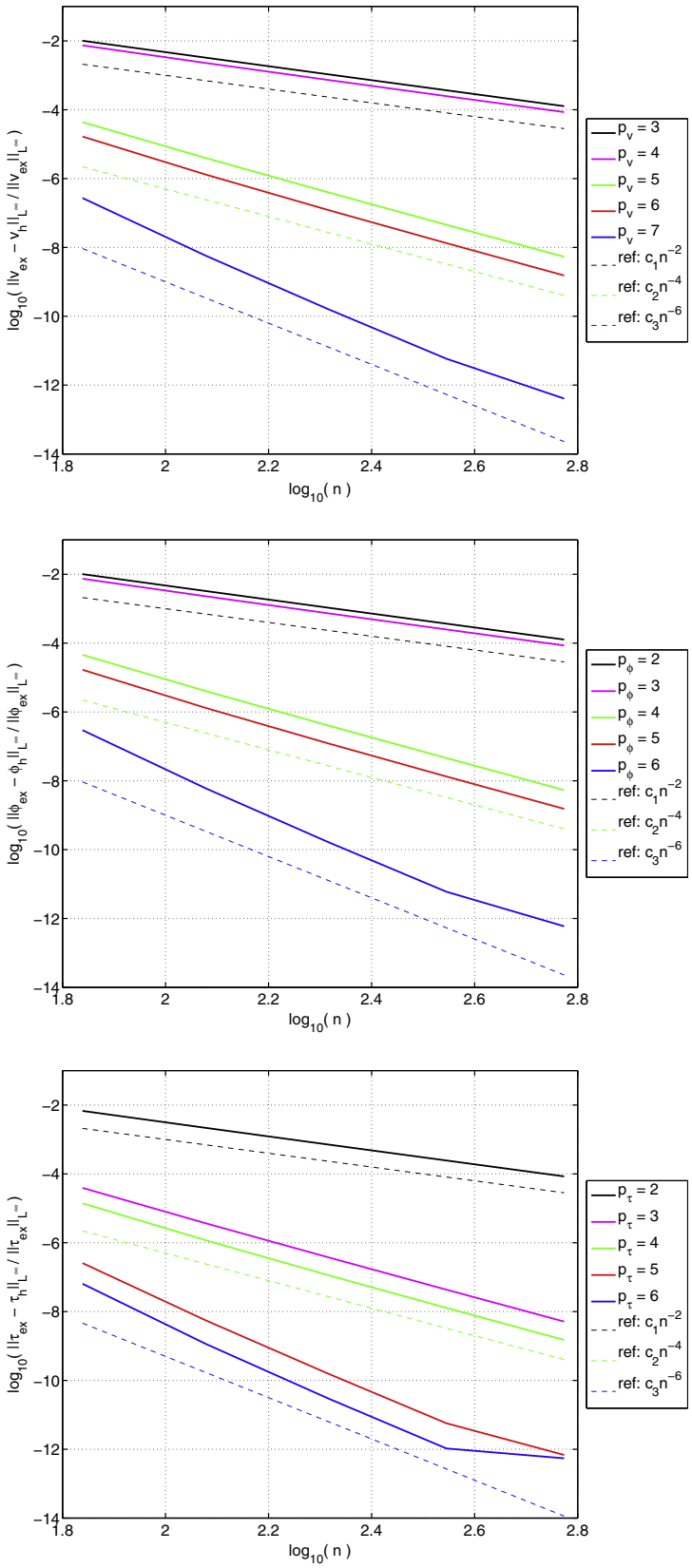

Fig. 2. Mixed collocation method with $p_\varphi = p_\tau = p_v - 1$. Relative errors versus number of total collocation points, for v (top), φ (middle), τ (bottom).

Noting that there exist $c_1 > 0$ and $c_2 > 0$ such that $c_1 \leqslant c(t) \leqslant c_2$, from (40) we get the error estimate, for all $s \in \mathbb{R}$:

$$\|\tilde{\varphi} - \tilde{\varphi}_h\|_{W^{s,\infty}} + \|\tilde{\nu} - \tilde{\nu}_h\|_{W^{s,\infty}} + \|\tilde{\tau} - \tilde{\tau}_h\|_{W^{s,\infty}} \leqslant C(s)|\nu_0(a) - \nu_{0,h}(a)| \leqslant C(s)\|\nu_0 - \nu_{0,h}\|_{L^\infty}, \tag{41}$$

where ν_0 and $\nu_{0,h}$ are the solutions to problems (25) and (28), respectively.

5.4. Error estimates

It is now straightforward to obtain the following error estimate, uniform in the thickness parameter t, for the error of the proposed collocation method.

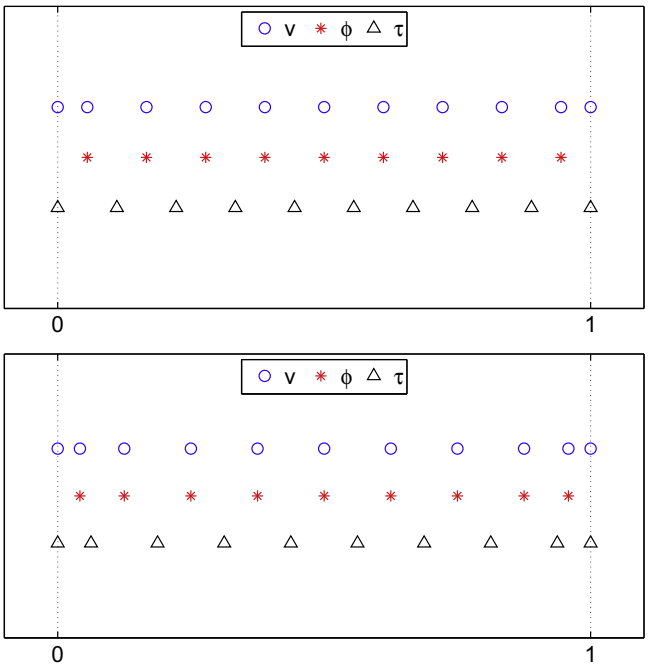

Fig. 3. Mixed collocation method with $p_\varphi = p_\tau = p_\nu - 1$. Distribution of the active collocation points relative to the spaces for ν, φ, and τ according to (49), for the choices $p_\nu = 3$ (top) and $p_\nu = 4$ (bottom) and a total of 30 active collocation points.

Theorem 5.1. *Let (φ, ν, τ) and $(\varphi_h, \nu_h, \tau_h)$ represent the solutions of problem (7) and (20), under Assumption 5.1 on the collocation points. Then it holds*

$$\|\varphi - \varphi_h\|_{W^{2,\infty}} + \|\nu - \nu_h\|_{W^{1,\infty}} + \|\tau - \tau_h\|_{W^{1,\infty}} \leqslant Ch^\beta |q|_{W^{\beta,\infty}} \tag{42}$$

with

$$\beta = \min(p_\nu, p_\tau, p_\varphi - 1), \tag{43}$$

and where the constant C is independent of the knot vectors and the thickness parameter t.

Proof. The proof immediately follows recalling (30) and by combining bound (41) with (31), (35), (37). Note that we also use $|\tau_0|_{W^{\beta+1,\infty}} \leqslant |q|_{W^{\beta,\infty}}$ (see $(25)_1$). □

Approximation results in higher order norms can also be easily obtained by using inverse estimates. Moreover, note that one could also extend the above results to the case of less regular loads q, which would possibly give a lower convergence rate β. We will not provide details of these extensions, since they take advantage of standard techniques. We also remark that Eq. (43) *should not be intended as a recipe* to find the optimal balancing among p_ν, p_ν and p_{tau}. Indeed, our estimates are not sharp, and, therefore, the *optimal* balancing is not necessarily driven by (43), i.e., a choice different from $p_\nu = p_\tau = p_\varphi - 1$ could possibly lead to better results.

The optimal selection of points for interpolation of one-dimensional splines is addressed in various papers. The only choice proved to be stable (i.e., satisfying Assumption 5.1) for any mesh and degree, are the so-called Demko abscissae proposed in [18]. These points are the extrema of suitable Chebyshev splines and can be obtained by an iterative algorithm (see for instance [16]). A different approach proposed in the engineering literature [22] is to collocate at the Greville abscissae, obtained as knot averages [16,18]. Although Greville abscissae interpolation is proved to be stable only up to degree 3, in practice this choice yields stable and accurate results in most situations. We refer to [3] for a deeper investigation and comparison between the Demko and Greville choices.

Remark 5.2. The result in Theorem 5.1 is surprising, at least in comparison with Galerkin schemes. Indeed, Theorem 5.1 shows a converge estimate, uniform in the thickness parameter, without requiring any particular compatibility condition among the three discrete spaces Φ_h, V_h, and Γ_h. In other words, the method is

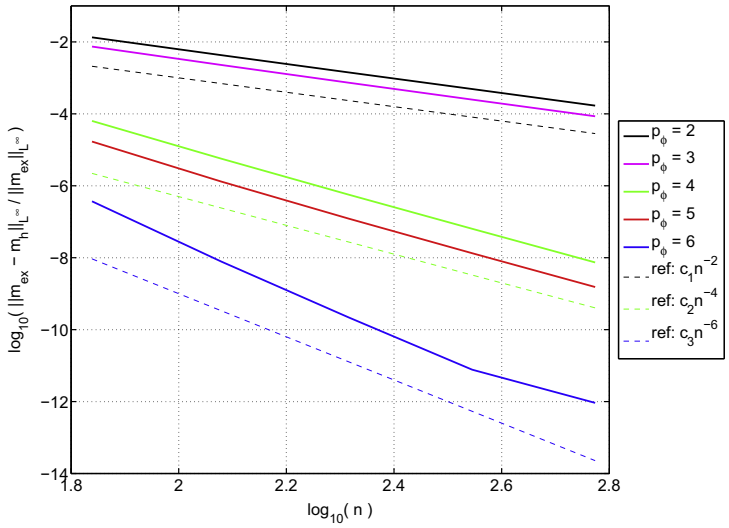

Fig. 4. Mixed collocation method with $p_\varphi = p_\tau = p_\nu - 1$. Relative errors versus number of total collocation points for the normalized bending moment m.

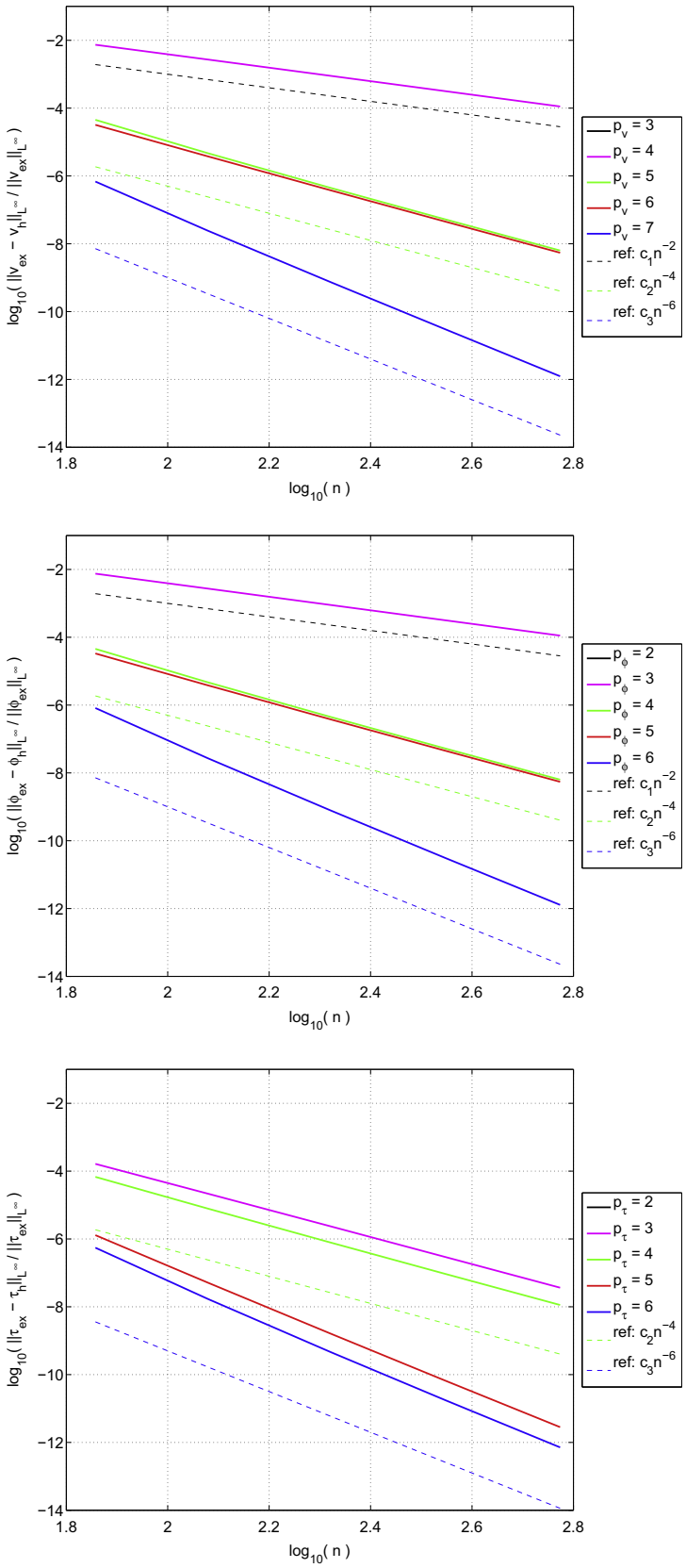

Fig. 5. Mixed collocation method with $p_\varphi = p_\tau = p_v - 1$, in the case of reduced inter-element continuity. Relative errors versus number of total collocation points, for v (top), φ (middle), τ (bottom).

locking-free regardless of the chosen polynomial degrees and space regularities. Even different meshes can be adopted among the three spaces. This is a very significant difference from typical Galerkin approaches where the discrete spaces Φ_h, V_h, Γ_h must be *carefully*

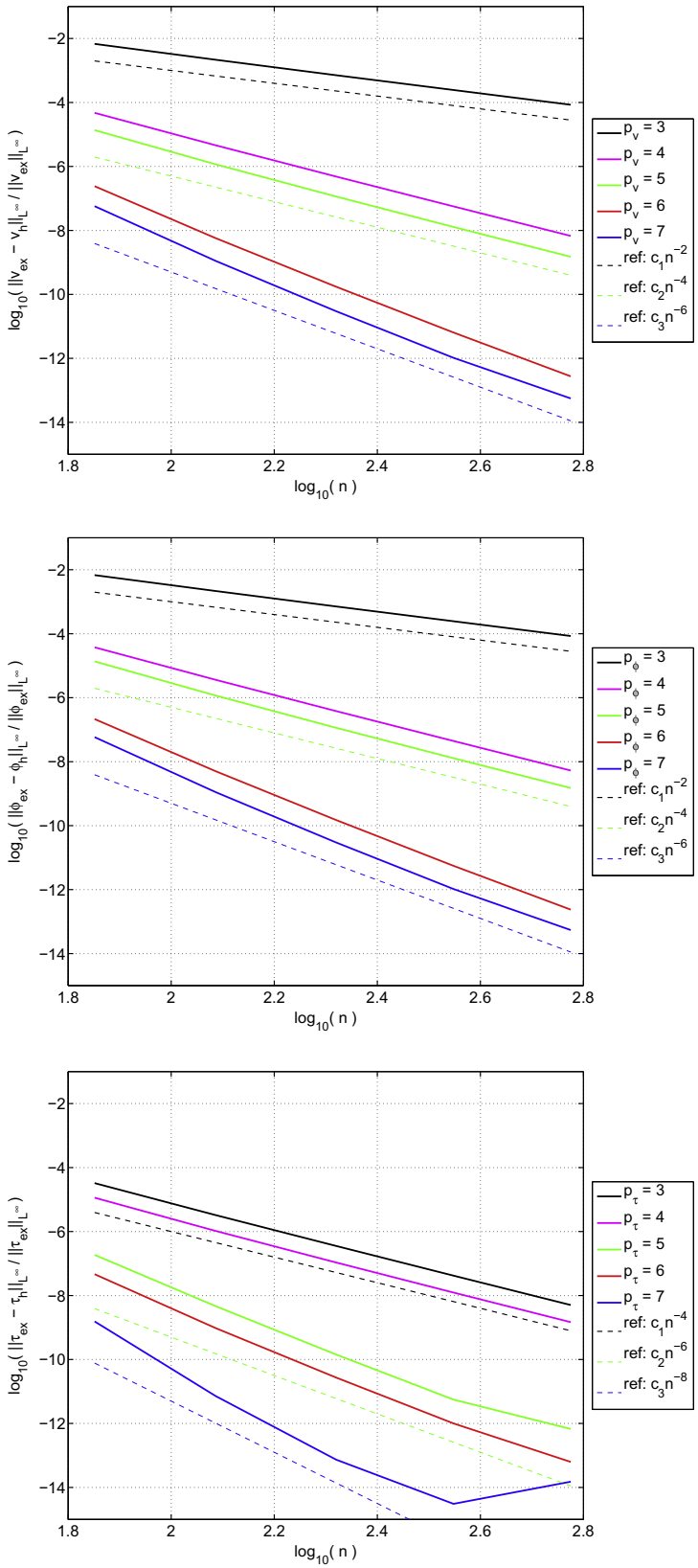

Fig. 6. Mixed collocation method with $p_\varphi = p_\tau = p_v$. Relative errors versus number of total collocation points, for v (top), φ (middle), τ (bottom).

chosen, to avoid the locking phenomenon and the occurrence of spurious modes. The numerical tests of Section (6) confirm this very appealing property of the proposed isogeometric collocation methods.

5.4.1. Equivalence between mixed and displacement-based methods

In some cases, the mixed collocation method (20) is equivalent to a displacement-based collocation method of the form (23). This occurs when it holds:

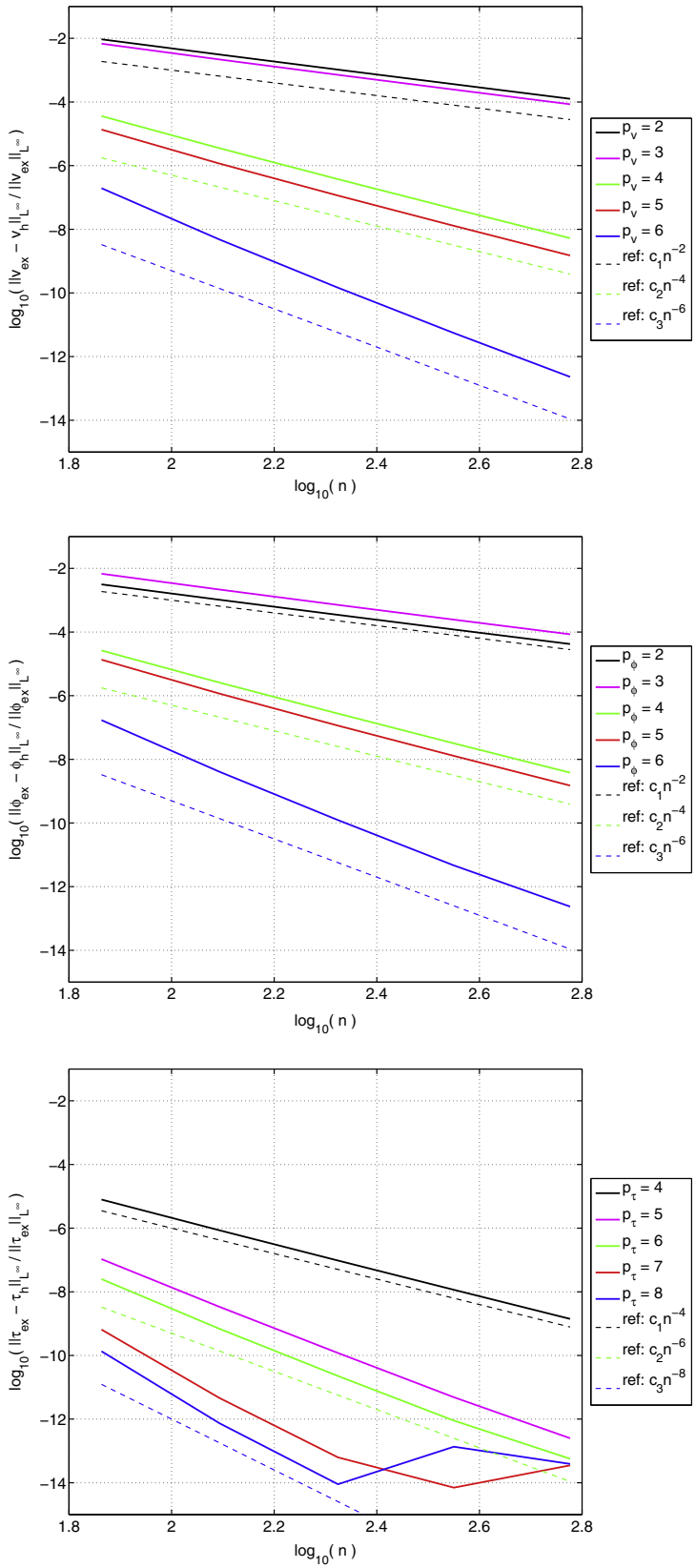

Fig. 7. Mixed collocation method with $p_\varphi = p_v = p_\tau - 2$. Relative errors versus number of total collocation points, for v (top), φ (middle), τ (bottom).

$$\Phi_h \subseteq V_h\prime \quad \text{and} \quad \Gamma_h = V_h\prime. \tag{44}$$

Indeed, from Eq. $(20)_3$ we obtain

$$v_h\prime = \left(-\varphi_h + \alpha^{-1} t^2 \tau_h\right)_{III}. \tag{45}$$

If (44) holds, from (45) we infer

$$v_h\prime = -\varphi_h + \alpha^{-1}t^2\tau_h. \tag{46}$$

Hence, we get

$$\tau_h = \alpha t^{-2}(v_h\prime + \varphi_h). \tag{47}$$

Substituting into(20)$_{1,2}$ Eq. (47) (i.e., eliminating τ_h), and noticing that $\Gamma_h' = V_h\prime\prime$, we obtain

$$\begin{cases} \text{Find } (\varphi_h, v_h) \in \Phi_h \times V_h \text{ such that :} \\ t^{-2}\left(v_h''(w_j) + \varphi_h'(w_j)\right) = q(w_j), & x_j \in \mathcal{N}(V_h') \\ -\varphi_h''(y_k) + \alpha t^{-2}\left(v_h'(y_k) + \varphi_h(y_k)\right) = 0, & y_k \in \mathcal{N}(\Phi_h'') \\ v_h(a) = v_h(b) = 0, \\ \varphi_h(a) = \varphi_h(b) = 0. \end{cases} \tag{48}$$

Above, we have defined $\mathcal{N}(V_h') := (\mathcal{N}(\Gamma_h')$, i.e., the collocation points associated with the space V_h'' are exactly the ones associated with the space Γ_h''.

6. Numerical results

In this section, we present some numerical experiments supporting the theoretical results previously provided. In particular, we consider the problem described by Eq. (7) (or, equivalently, Eq. (9)) and we select as the problem domain the interval $[0,1]$ (i.e., $a = 0$ and $b = 1$). We then choose the loading function:

$$q(x) = -\frac{8\pi^3}{\alpha}\cos(2\pi x),$$

giving rise to the analytical solution:

$$\begin{cases} v(x) = \frac{4\pi^2 t^{2/\alpha+1}}{2\pi}(\cos(2\pi x) - 1); \\ \varphi(x) = \sin(2\pi x); \\ \tau(x) = -4\pi^2\sin(2\pi x). \end{cases}$$

In all presented numerical examples, we adopt the following model parameters: $\alpha = 4$ and $t = 10^{-4}$.

We moreover remark that we assume maximum inter-element regularity (i.e., no internal knot repetitions) in most of the considered tests, and we explicitly specify the adopted regularity only when this is reduced by means of knot repetitions. In all the presented tests we restrict ourselves to the case where all knot vectors induce the same mesh, i.e., $\mathcal{M}_{h_\varphi} \equiv \mathcal{M}_{h_v} \equiv \mathcal{M}_{h_\tau}$, see Remark 4.2. Finally, note that in all the mixed tests we follow formulation (20).

The model problem described above is then solved using different choices of mixed or displacement-based collocation formulations and the obtained results are reported and commented in

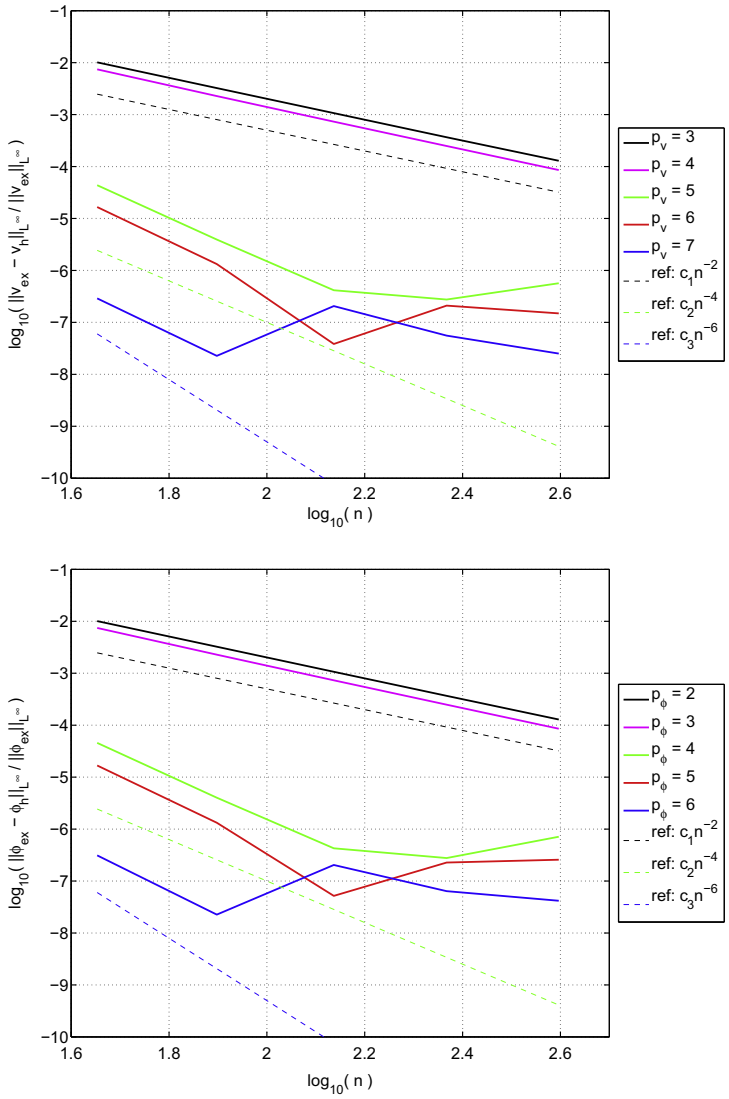

Fig. 8. Displacement-based collocation method with $p_\varphi = p_v - 1$. Relative errors versus number of total collocation points, for v (top) and φ (bottom).

the following sections. All results are presented, for several choices of p_v, in terms of convergence plots of the problem variable relative errors versus the number of total active collocation points (indicated with n in the figures). Errors are computed in L^∞-norm and are normalized with respect to the norm of the analytical solution.

In the presented numerical tests we have chosen the following collocation points in the spirit of [3]. Such points are first defined in the parametric space and then mapped to the physical space through the mapping F. Referring to (10), (13), and (15), we set

$$\begin{aligned} x_j &= F(\widehat{x}_j), \quad \widehat{x}_j = \frac{\xi^\varphi_{j+2} + \xi^\varphi_{j+3} + \cdots + \xi^\varphi_{j+p_\varphi+1}}{p_\varphi}, \quad j = 1,2,\ldots,n_\varphi, \\ y_k &= F(\widehat{y}_k), \quad \widehat{y}_k = \frac{\xi^v_{k+2} + \xi^v_{k+3} + \cdots + \xi^v_{k+p_v}}{p_v - 1}, \quad k = 1,2,\ldots,n_v, \\ z_i &= F(\widehat{z}_i), \quad \widehat{z}_i = \frac{\xi^\tau_{i+2} + \xi^\tau_{i+3} + \cdots + \xi^\tau_{i+p_\tau}}{p_\tau - 1}, \quad i = 1,2,\ldots,n_\tau \end{aligned} \tag{49}$$

We remark that the abscissae $\{y_k\}$ and $\{z_j\}$ are the standard Greville abscissae associated to the derivative spaces V_h' and τ_h', respectively. On the contrary, the abscissae $\{x_j\}$ are the Greville abscissae associated to the space Φ_h, dropping the first and last points (for boundary condition imposition). As an alternative, the Greville abscissae associated with the second derivative space Φ_h'' can be used (but this choice does not significantly affect the numerical results).

6.1. Mixed collocation methods: $p_\varphi = p_\tau = p_v - 1$

We start considering a mixed collocation method where we select $p_v = p_\tau = p_v - 1$. The results obtained in this case are reported in Fig. 2 and are in agreement with our theoretical results. In particular, no locking behavior is observed for any degree choice (despite the small adopted thickness parameter, $t = 10^{-4}$).

We remark that for $p_v = 7$, it is not possible to obtain the correct convergence slope below an error level of 10^{-12}, since this is the minimum error level that can be computed in a reliable way, given the condition number of the stiffness matrix (that for $p_v = 7$ may reach the order of 10^5). Analogous considerations hold also for the numerical experiments of the following sections.

Finally, for the case under consideration (i.e., $p_\varphi = p_\tau = p_v - 1$), the plots of the distribution of the active collocation points relative to the spaces for v, φ, and τ according to (49), for the choices $p_v = 3, 4$ and a total of 30 active collocation points, are reported in Fig. 3.

6.1.1. Approximation of bending moment

In engineering applications, the approximation of beam bending moments is of paramount importance; in this section we discuss this issue and we show the convergence behavior of such an important quantity within the proposed isogeometric collocation scheme.

In the elastic beam theory, the bending moment is expressed in terms of the cross section rotation as follows

$$M(x) = EI\varphi'(x), \tag{50}$$

and a normalized bending moment can be written as

$$m(x) = M(x)\frac{b-a}{EI} = (b-a)\varphi'(x). \tag{51}$$

Therefore, the L^∞-norm of the bending moment is proportional to the $W^{1,\infty}$-norm (i.e., the L^∞-norm of the first derivative) of the cross section rotation $\varphi(x)$. In [3], it is shown that the same convergence rates in both L^∞- and $W^{1,\infty}$-norm are attained for the solution of second-order partial differential equations, when isogeometric collocation schemes are employed for the approximation. As a conse-

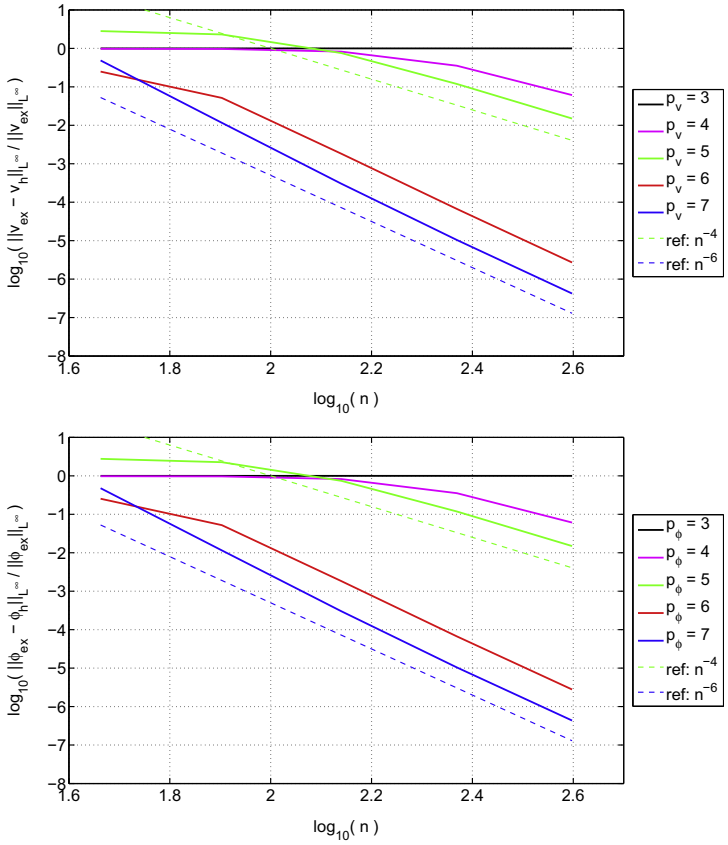

Fig. 9. Displacement-based collocation method with $p_\varphi = p_v$. Relative errors versus number of total collocation points, for v (top) and φ (bottom).

quence, *the same convergence behavior for cross section rotations and bending moments is in general expected*.

In Fig. 4, we report the bending moment convergence rates in L^∞-norm for the example presented above; as expected, the same convergence rates obtained for rotations (see Fig. 2) are obtained. We remark that analogous results can be attained for all the examples of the following sections, but they are not reported for the sake of brevity.

6.1.2. Case of reduced inter-element continuity

In order to test the method in case of reduced inter-element continuity, we perform the numerical experiments above also adopting knot vectors with repeated internal knots. In this way, inter-element continuity drops to C^{p-2}, being p the degree of the approximation. The obtained results are reported in Fig. 5, where it is possible to appreciate the same behavior, in terms of convergence rates, as in the case of maximum regularity.

We highlight that in this numerical test we select $p_v = 4$ as minimum degree for v. The reason for this choice is that $p_v = 3$ would lead to a C^0 quadratic approximation for φ, that cannot work since the second derivative of φ appears in the second equation of system (7). As a general remark, the case of C^0 discrete spaces and/or jumps in the material or loading data could be treated (for instance) using a multipatch approach, that is beyond the scope of the present paper. For a deeper investigation of the multipatch case for isogeometric collocation see [4].

Remark 6.1. We have also studied in detail the behavior of the method with respect to different choices of the thickness parameter t. In particular, we have considered values of t equal to $10^{-1}, 10^{-2}, 10^{-3}, 10^{-4}, 10^{-5}$, and 10^{-6}, and no sensible differences have been evidenced in terms of error convergence plots among the different choices.

6.2. Mixed collocation methods: $p_\varphi = p_\tau = p_v$ and $p_\varphi = p_v = p_\tau - 2$

We now consider other possible choices of mixed collocation methods. In particular we study the case of equal approximation for all variables, namely, $p_\varphi = p_\tau = p_v$, and a more "exotic" case, where we select $p_\varphi = p_v = p_\tau - 2$. This is to check that, as predicted by our theory, for any choice of the degree approximations a good solution is provided and no locking occurs. The results obtained for these two cases are reported, respectively, in Figs. 6 and 7, both showing results similar to those of the previous section.

6.3. Displacement-based collocation methods

We finally test the behavior of displacement-based collocation methods. In particular, we consider the two cases $p_\varphi = p_v - 1$ and $p_\varphi = p_v$; the obtained results are reported, respectively, in Figs. 8 and 9.

Fig. 8 shows, for the choice $p_\varphi = p_v - 1$, numerical results in agreement with our theory. In particular, no locking behavior is observed for any degree choice. However, the high condition number of the stiffness matrix significantly affects the results when high orders are employed and an error level of 10^{-7} is attained.

Fig. 9, instead, shows that the choice $p_\varphi = p_v$ leads to locking for low order approximations.

7. Conclusions

We have considered an isogeometric collocation approach for the approximation of initially straight planar Timoshenko beams. The proposed schemes, based on a standard mixed formulation of the problem, are shown, theoretically and computationally, to be *free of shear locking, without the need of any compatibility condition among the chosen discrete spaces*. This very appealing feature, in contrast with most of the Galerkin approximation procedures (Finite Element Methods, for instance), opens the possibility to design simple and efficient numerical schemes for other more complicated thin structures.

Acknowledgments

The authors were partially supported by the European Commission through the FP7 Factory of the Future project *TERRIFIC* (FoF-ICT-2011.7.4, Reference: 284981). L. Beirão da Veiga and A. Reali were also partially supported by the European Research Council through the FP7 Ideas Starting Grants nos. 259229 *ISOBIO* and 205004 *GeoPDEs*, as well as by the Italian MIUR through the FIRB "Futuro in Ricerca" Grant RBFR08CZ0S. This support is gratefully acknowledged.

References

[1] I. Akkermann, Y. Bazilevs, V.M. Calo, T.J.R. Hughes, S. Hulshoff, The role of continuity in residual-based variational multiscale modeling of turbulence, Comput. Mech. 41 (2008) 371–378.
[2] F. Auricchio, L. Beirão da Veiga, A. Buffa, C. Lovadina, A. Reali, G. Sangalli, A fully "locking-free" isogeometric approach for plane linear elasticity problems: a stream function formulation, Comput. Methods Appl. Mech. Engrg. 197 (2007) 160–172.
[3] F. Auricchio, L. Beirão da Veiga, T.J.R. Hughes, A. Reali, G. Sangalli, Isogeometric collocation methods, Math. Models Methods Appl. Sci. 20 (2010) 2075–2107.
[4] F. Auricchio, L. Beirão da Veiga, T.J.R. Hughes, A. Reali, G. Sangalli, Isogeometric collocation for elastostatics and explicit dynamics. Comput. Methods Appl. Mech. Engrg., in press. <http://dx.doi.org/10.1016/j.cma.2012.03.026>.
[5] F. Auricchio, L. Beirão da Veiga, C. Lovadina, A. Reali, The importance of the exact satisfaction of the incompressibility constraint in nonlinear elasticity: mixed FEMs versus NURBS-based approximations, Comput. Methods Appl. Mech. Engrg. 199 (2010) 314–323.
[6] F. Auricchio, F. Calabró, T.J.R. Hughes, A. Reali, G. Sangalli, A simple algorithm for obtaining nearly optimal quadrature rules for NURBS-based isogeometric analysis, Comput. Methods Appl. Mech. Engrg., in press. <http://dx.doi.org/10.1016/j.cma.2012.04.014>.
[7] Y. Bazilevs, L. Beirão da Veiga, J.A. Cottrell, T.J.R. Hughes, G. Sangalli, Isogeometric analysis: approximation, stability and error estimates for h-refined meshes, Math. Models Methods Appl. Sci. 16 (2006) 1–60.
[8] Y. Bazilevs, C. Michler, V.M. Calo, T.J.R. Hughes, Weak Dirichlet boundary conditions for wall-bounded turbulent flows, Comput. Methods Appl. Mech. Engrg. 196 (2007) 4853–4862.
[9] Y. Bazilevs, V.M. Calo, J.A. Cottrell, T.J.R. Hughes, A. Reali, G. Scovazzi, Variational multiscale residual-based turbulence modeling for large eddy simulation of incompressible flows, Comput. Methods Appl. Mech. Engrg. 197 (2007) 73–201.
[10] L. Beirão da Veiga, A. Buffa, J. Rivas, G. Sangalli, Some estimates for h-p-k-refinement in isogeometric analysis, Numer. Math. 118 (2011) 271–305.
[11] L. Beirão da Veiga, A. Buffa, C. Lovadina, M. Martinelli, G. Sangalli, An isogeometric method for the Reissner–Mindlin plate bending problem, Comput. Methods Appl. Mech. Engrg. 209–212 (2012) 45–53.
[12] L. Beirão da Veiga, D. Cho, G. Sangalli, Anisotropic NURBS approximation in isogeometric analysis, Comput. Meth. Appl. Mech. Engrg. 209–212 (2012) 1–11.
[13] J.A. Cottrell, T.J.R. Hughes, Y. Bazilevs, Isogeometric Analysis, Towards integration of CAD and FEA, Wiley, 2009.
[14] J.A. Cottrell, A. Reali, Y. Bazilevs, T.J.R. Hughes, Isogeometric analysis of structural vibrations, Comput. Meth. Appl. Mech. Engrg. 195 (2006) 5257–5296.
[15] J.A. Cottrell, T.J.R. Hughes, A. Reali, Studies of refinement and continuity in isogeometric structural analysis, Comput. Meth. Appl. Mech. Engrg. 196 (2007) 4160–4183.
[16] C. de Boor, A Practical Guide to Splines, Springer, 2001.
[17] C. de Falco, A. Reali, R. Vázquez, GeoPDEs: a research tool for IsoGeometric analysis of PDEs, Adv. Engrg. Softw. 42 (2011) 1020–1034.
[18] S. Demko, On the existence of interpolation projectors onto spline spaces, J. Approximat. Theory 43 (1985) 151–156.
[19] T.J.R. Hughes, J.A. Cottrell, Y. Bazilevs, Isogeometric analysis: CAD finite elements NURBS exact geometry and mesh refinement, Comput. Methods Appl. Mech. Engrg. 194 (2005) 4135–4195.
[20] T.J.R. Hughes, A. Reali, G. Sangalli, Duality and unified analysis of discrete approximations in structural dynamics and wave propagation: comparison of *p*-method finite elements with *k*-method NURBS, Comput. Methods Appl. Mech. Engrg. 197 (2008) 4104–4124.

[21] T.J.R. Hughes, A. Reali, G. Sangalli, Efficient quadrature for NURBS- based isogeometric analysis, Comput. Methods Appl. Mech. Engrg. 199 (2010) 301–313.
[22] R.W. Johnson, A B-spline collocation method for solving the incompressible Navier–Stokes equations using an ad hoc method: the boundary residual method, Comput. Fluids 34 (1) (2005) 121–149.
[23] A. Reali, An isogeometric analysis approach for the study of structural vibrations, J. Earthquake Engrg. 10 (2006) 1 1–30.
[24] S.P. Timoshenko, On the correction factor for shear of the differential equation for transverse vibrations of bars of uniform cross-section, Phil. Mag. 41 (1921) 744–746.
[25] Y. Zhang, Y. Bazilevs, S. Goswami, C.L. Bajaj, T.J.R. Hughes, Patient-specific vascular NURBS modeling for isogeometric analysis of blood flow, Comput. Methods Appl. Mech. Engrg. 196 (2007) 2943–2959.